

# Thermoelectric Properties of $\beta$ -Zn<sub>4</sub>Sb<sub>3</sub> Synthesized by Mechanical Alloying and Pulse Discharge Sintering

Takashi Itoh,\* Jiayi Shan,<sup>†</sup> and Kuniyuki Kitagawa<sup>‡</sup>  
Nagoya University, Chikusa-ku, Nagoya 464-8603, Japan

DOI: 10.2514/1.20944

Thermoelectric power generation is a helpful method for harnessing waste thermal energy, particularly covering a middle temperature range between 500 and 800 K. A  $\beta$ -Zn<sub>4</sub>Sb<sub>3</sub> compound has become the focus of attention as a thermoelectric material applicable to thermoelectric power generation around 700 K. In this research, a method combining the mechanical alloying with the pulse discharge sintering was adopted to obtain the sintered compact of  $\beta$ -Zn<sub>4</sub>Sb<sub>3</sub>. Pure zinc and antimony powders were used as the starting material for mechanical alloying. These powders were mixed in the stoichiometry ratio of 4 to 3, or more Zn-rich. The mechanical alloying was carried out by planetary ball milling under conditions of fixed revolution speed and variable milling time. The influence of the milling time on the synthesis of  $\beta$ -Zn<sub>4</sub>Sb<sub>3</sub> was investigated. The sintering was executed at two sintering temperatures and under fixed conditions of sintering time, pressing pressure, and atmosphere. The influences of the sintering temperature of pulse discharge sintering on the polycrystalline grain size and the thermoelectric properties were also studied. The following results were clarified. The phases of ZnSb and Zn are easily obtained by mechanical alloying for 50 h or longer time. These phases change to a single phase of  $\beta$ -Zn<sub>4</sub>Sb<sub>3</sub> through pulse discharge sintering under the optimum condition of Zn-rich mixing. The sintered compact of  $\beta$ -Zn<sub>4</sub>Sb<sub>3</sub> with 1.17 of nondimensional figure of merit can be obtained at 673 K with the proposed mechanical alloying with pulse discharge sintering method.

## Nomenclature

- $D$  = polycrystalline grain size, m  
 $K$  = Scherrer constant  
 $L_0$  = Lorentz number, V<sup>2</sup>K<sup>-2</sup>  
 $T$  = absolute temperature, K  
 $ZT$  = thermoelectric (nondimensional) figure of merit  
 $\alpha$  = Seebeck coefficient, VK<sup>-1</sup>  
 $\beta$  = full width at half-maximum of x-ray diffraction peak at diffraction angle  $\theta$ , rad  
 $\theta$  = diffraction angle, rad  
 $\kappa$  = thermal conductivity, Wm<sup>-1</sup>K<sup>-1</sup>  
 $\kappa_E$  = electron thermal conductivity, Wm<sup>-1</sup>K<sup>-1</sup>  
 $\kappa_L$  = lattice thermal conductivity, Wm<sup>-1</sup>K<sup>-1</sup>  
 $\lambda$  = wavelength of x-ray source, m  
 $\rho$  = electrical resistivity,  $\Omega$ m

## I. Introduction

IN MOST current energy systems, 30–70% of the primary or chemical energy originating from fossil fuels such as petroleum, natural gas, and coal is not used and is wasted during the energy conversion. It is very important from a standpoint of saving energy to generate electricity from such waste-heat resources. Thermoelectric power generation systems are solid apparatuses constructed with thermoelectric semiconductors and they can directly convert the heat energy into electrical energy. Thermoelectric devices are therefore promising to generate electricity from various heat resources such as automobiles, cogeneration systems, and waste material incinerators.

Presented as Paper 5564 at the 2nd International Energy Conversion Engineering Conference, Providence, RI, 16–19 August 2004; received 7 November 2005; revision received 23 March 2007; accepted for publication 31 July 2007. Copyright © 2007 by the American Institute of Aeronautics and Astronautics, Inc. All rights reserved. Copies of this paper may be made for personal or internal use, on condition that the copier pay the \$10.00 per-copy fee to the Copyright Clearance Center, Inc., 222 Rosewood Drive, Danvers, MA 01923; include the code 0748-4658/08 \$10.00 in correspondence with the CCC.

\*Associate Professor, Division of Integrated Research Projects, EcoTopia Science Institute.

<sup>†</sup>Postdoctoral Fellow, Division of Energy Science, EcoTopia Science Institute.

<sup>‡</sup>Professor, Division of Energy Science, EcoTopia Science Institute. Senior Member AIAA.

The exhaust heat from various energy systems has a middle range of temperature (600–800 K). A development of high-performance thermoelectric materials applicable in this middle range of temperature is thus indispensable to realize the thermoelectric power generation systems for routine use.

It has been known that the Zn–Sb system includes the compounds of ZnSb, Zn<sub>3</sub>Sb<sub>2</sub>,  $\alpha$ -Zn<sub>4</sub>Sb<sub>3</sub>,  $\beta$ -Zn<sub>4</sub>Sb<sub>3</sub>, and  $\gamma$ -Zn<sub>4</sub>Sb<sub>3</sub>. Soma et al. [1] studied the thermoelectric properties of the  $\alpha$ -Zn<sub>4</sub>Sb<sub>3</sub> compound in the temperature range of 4 to 260 K. The  $\beta$ -Zn<sub>4</sub>Sb<sub>3</sub> compound has attracted increasing attention as a thermoelectric material applicable to thermoelectric power generation around 700 K, because Caillat et al. [2] reported that the sintered compact of this compound has a very low thermal conductivity, an excellent performance, and that the maximum nondimensional figure of merit  $ZT$  is 1.3 at 670 K. Yamamoto et al. [3] successfully synthesized the  $\beta$ -Zn<sub>4</sub>Sb<sub>3</sub> compound by bulk mechanical alloying (BMA) and obtained the maximum  $ZT$  of 1.0 at 680 K. Recently, Ohzora et al. [4] succeeded in preparing the compound having the excellent  $ZT$  of 1.6 through an optimum sintering process. Here, the nondimensional figure of merit is defined as follows.

$$ZT \equiv \frac{\alpha^2 T}{\kappa \rho} \quad (1)$$

The recent studies on the  $\beta$ -Zn<sub>4</sub>Sb<sub>3</sub> compound are summarized in Table 1. This table includes data of the mole ratio of Zn to Sb, the production process used in the study, and the maximum figure of merit  $ZT_{\max}$ .

The mechanical alloying (MA) method is a material processing technique for assembling metal constituents with a controlled microstructure by the repeated welding, fracturing, and rewelding of a mixture of powder particles, and it is useful for synthesizing intermetallic compounds. Pulse discharge sintering (PDS), alias spark plasma sintering, is a kind of hot pressing method that has an advantage of rapid and activating sintering at relatively low temperatures. The MA–PDS method combining MA with PDS is powerful for promoting the synthesis of desired compounds and for creating a sintered body, with the fine microstructure giving a decrease of thermal conductivity and an improvement of material strength. In this study, we attempted to synthesize the  $\beta$ -Zn<sub>4</sub>Sb<sub>3</sub> compound with this MA–PDS method as a new manufacturing process, replacing the traditional melting, crushing, and sintering

**Table 1** Recent studies on  $\beta$ -Zn<sub>4</sub>Sb<sub>3</sub>

Researchers	Mole ratio Zn/Sb	Production process <sup>a</sup>	$ZT_{\max}$
Caillat et al. [2]	4/3	Melting (1023 K, 2 h) to crushing to HP to HT (673 K, 5 days)	1.3 (670 K)
Yamamoto et al. [3]	4/3, 4.1/3, 4.19/3, 4.29/3	BMA to HT (623 K, 5 h) to HP (773 k, 100 MPa, 5 h)	1.0 (680 K)
Ohzora et al. [4]	4.03/3	Melting to crushing to HP (673 K, 743 K, 39.2 MPa, 5 h) to HT (523 K, 100 h)	1.6 (673 K)
Zhang et al. [5]	3/3, 3.82/3, 3.98/3, 4.27/3, 7/3	Melting (1023 K, 2 h) to crushing to HP (733 K, 50–60 MPa, 3 h)	1.3 (673 K)

<sup>a</sup>HP is hot pressing, HT is heat treatment, and BMA is bulk mechanical alloying.

methods for achieving an excellent thermoelectric performance. The mixing mole ratio of zinc to antimony powders, the milling time in MA, and the sintering temperature are changed. Influences of these factors on synthesized phases and on their thermoelectric properties are investigated. The syntheses of  $\beta$ -Zn<sub>4</sub>Sb<sub>3</sub> were confirmed reproducibly by x-ray diffraction (XRD) analysis. The thermoelectric properties were measured and the optimum conditions of MA and PDS were examined.

## II. Experimental

### A. Sample Powders and Mixing Ratio

The commercially available zinc powder (purity of 99.9% and size of less than 75  $\mu\text{m}$ ) and antimony powder (purity of greater than 99.9% and size of less than 45  $\mu\text{m}$ ) were used as starting powders. The two powders were blended in a stoichiometric mole ratio of  $\beta$ -Zn<sub>4</sub>Sb<sub>3</sub> (Zn/Sb = 4/3) and in several Zn-rich mole ratios (Zn/Sb = 4.03/3, 4.06/3, 4.09/3, 4.12/3, and 4.15/3). The mixed powders of 30 g were weighed out.

### B. Mechanical Alloying

A zirconia pot (capacity of 500 ml) and zirconia balls (diameter of 5 mm) were used for mechanical alloying. A weight ratio of powder to balls was 1/20. The 0.5 mass % hexane was added to the pot for preventing adhesion of the powder on the surfaces of the pot and balls during the mechanical alloying process. After substituting argon gas into the pot and making the pot airtight, the mechanical alloying process was carried out under conditions of a fixed rotation speed of 150 rpm and different milling times of 0, 50, 75, 100, 200, and 300 h, by using planetary ball milling equipment (P-5, Fritsch Japan Co. Ltd.). Subsequently, the pot was opened in a globe box filled with argon gas and the resulting MA powders were collected in the atmosphere.

### C. Pulse Discharge Sintering

The MA powders were sintered in pulse discharge sintering equipment (SPS-1050, SPS Syntex, Inc.). The procedure is as follows. The MA powder was packed into a cylindrical graphite container (20-mm i.d., 40-mm o.d., and 40 mm in height). The packed powder was sandwiched between graphite punches under a compression pressure of 1 MPa, heated to 473 K, and dried for 10 min in vacuum. Subsequently, the powder was compressed under

40 MPa, sintered at 673, 723, or 753 K for 20 min in vacuum or argon atmosphere, and then cooled down to the room temperature for 360 min. Disk-type sintered samples (20 mm in diameter and 5 mm in thickness) were made under various sintering conditions. The details of the temperature and compression pressure profiles used during pulse discharge sintering are shown in Fig. 1.

### D. Identification of Synthesized Phases and Estimation of Crystallite Size

The phases synthesized after MA and after PDS were identified by XRD analysis with Cu  $K\alpha$  radiation (RINT2500TTR, Rigaku Corporation). The crystallite sizes in the MA-powder sample and in the sintered sample were also estimated from the XRD analysis. The polycrystalline grain size of the sample was obtained according to the following equation (Scherrer's equation).

$$D = \frac{K\lambda}{\beta \cos \theta} \quad (2)$$

where the Scherrer constant  $K$  is 0.9 and the wavelength of the x-ray source  $\lambda$  is 0.15405 for Cu  $K\alpha$  radiation. The mean value of the size  $D$  obtained from five main x-ray diffraction peaks in each sample was used as a typical polycrystalline grain size. The value might lack accuracy in the grain size a little, but it is an effective value that can indicate the state of grain refining.

### E. Measurements of Thermoelectric Properties

After the sintered samples were cut into the prescribed shape, their Seebeck coefficient and electrical resistivity were measured with thermoelectric measuring equipment (ZEM-2, Ulvac-Riko, Inc.), based on steady direct-current and direct-current four-terminal methods, respectively. The thermal conductivity was measured with thermal-constant measuring equipment (TC-7000, Ulvac-Riko, Inc.), based on the laser-flash method.

### F. Outward Appearance Observation of Sintered Bodies

To survey the optimum sintering condition for making a sound or crack-free sintered body, the outward appearances of the sintered bodies made under various sintering conditions were observed and their images were taken by a digital camera. The MA powder was prepared by mechanically alloying the mixed powder (mole ratio Zn/Sb = 4.09/3) under the conditions of 150 rpm and 100 h. The samples for the observation were prepared by sintering the MA powder at 673, 723, or 753 K in vacuum or argon atmosphere.

## III. Results and Discussions

### A. Influences of Milling Time on Synthesized Phases and Polycrystalline Grain Size

The influences of milling time on x-ray diffraction patterns of the powders after MA (mole ratio Zn/Sb = 4/3) and of their bulk materials sintered at 723 K in argon atmosphere are shown in Figs. 2a and 2b, respectively. In the diffraction patterns after MA, the diffraction peak becomes broader after milling for the time longer than 75 h. The principal phases are ZnSb and Zn, regardless of the milling time. Though the synthesis of  $\beta$ -Zn<sub>4</sub>Sb<sub>3</sub> progressed after PDS, the phase of ZnSb still remains as the principal phase. In both MA powder and PDS-bulk material, the identified phases hardly change for milling times of 50 to 300 h. The identification results of the phases synthesized from the mixed powder (mole ratio

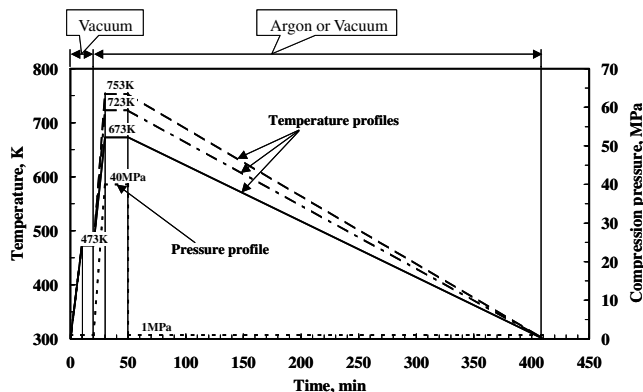


**Fig. 1** Temperature profiles and compression pressure profiles during PDS.



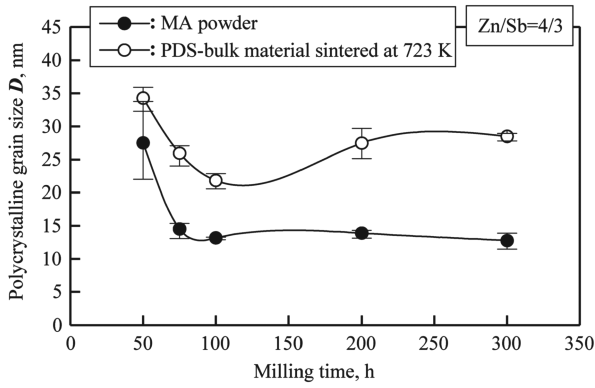


**Fig. 3** Influences of milling time on polycrystalline grain sizes of MA powder and PDS-bulk material sintered at 723 K.

observation of sintered bodies indicate that although the PDS process at 673 K makes a sound sintered body, the process maintains the fine polycrystalline grain size and the phases of the MA powder. Table 3 shows that the bulk material sintered at 673 K with the mole ratio Zn/Sb of 4.09/3 has the same principal phases of ZnSb and Zn as the MA powder, whereas the bulk material sintered at 723 K with the same mole ratio has the single phase of  $\beta$ -Zn<sub>4</sub>Sb<sub>3</sub>. These results seem to be related to the thermoelectric properties.

We confirmed that the reproducibility of measurement values of the thermoelectric properties in this study was maintained with a difference less than 5%. The temperature dependencies of the electrical resistivity for the samples sintered at 673 and 723 K are shown in Fig. 7. The sample sintered at 723 K keeps the electrical resistivity lower than that sintered at 673 K over the measurement temperature range. In general, the finer polycrystalline grain size leads to the higher electrical resistivity in the same materials. But the synthesized phase of the sample sintered at 673 K is also different from that sintered at 723 K in this case. Thus, the difference in the electrical resistivity is likely attributable to the differences in both the synthesized phases and the polycrystalline grain sizes.

Figure 8 shows the comparison between the Seebeck coefficients of the two samples sintered at the different temperatures. The Seebeck coefficient of the sample sintered at 723 K is higher than that sintered at 673 K over the measurement temperature range. The

Seebeck coefficient greatly depends on the materials. Thus, the difference of electrical resistivity at different sintering temperatures depends on whether the  $\beta$ -Zn<sub>4</sub>Sb<sub>3</sub> phase exists in the sintered body.

The temperature dependencies of thermal conductivity of two samples sintered at the different temperatures are shown in Fig. 9. The thermal conductivity of the sample sintered at 723 K maintains a lower level than that sintered at 673 K over the measurement temperature range. This can be explained by the fact that the  $\beta$ -Zn<sub>4</sub>Sb<sub>3</sub> phase has lower thermal conductivity than that of the ZnSb and Zn phases [5]. The thermal conductivity of thermoelectric materials is generally expressed as a total of the thermal conductivities due to the lattice and electronic contributions as follows.

$$\kappa = \kappa_L + \kappa_E \quad (3)$$

According to the Wiedemann–Franz Law, the electron thermal conductivity  $\kappa_E$  can be calculated as follows.

$$\kappa_E = \frac{L_0 T}{\rho} \quad (4)$$

where the Lorentz number  $L_0$  is  $2.45 \times 10^{-8} \text{ V}^2 \text{ K}^{-2}$ . The lattice thermal conductivity  $\kappa_L$  is estimated as a difference between the total thermal conductivity and the electron conductivity.

$$\kappa_L = \kappa - \kappa_E \quad (5)$$

Figure 10 shows the temperature dependencies of three types of thermal conductivities measured and calculated with Eqs. (4) and (5). The changes in these thermal conductivities of the samples sintered at 673 and 723 K are shown in Figs. 10a and 10b, respectively. The two types of samples sintered at the different temperatures have almost the same value change in the electron thermal conductivity. On the other hand, the lattice thermal conductivity of the sample sintered at 723 K is lower than that at 673 K over the measurement temperature range. It means that the phonon scattering in the  $\beta$ -Zn<sub>4</sub>Sb<sub>3</sub> compound (namely, the phonon glass material) is stronger than that of the phase mixture of ZnSb and Zn (see Table 3), significantly decreasing the lattice thermal conductivity in the higher temperature range.

It becomes clear that the sintering at high temperature (723 K) creates the  $\beta$ -Zn<sub>4</sub>Sb<sub>3</sub> compound, improving all thermoelectric properties and performance. The thermoelectric figure of merit  $ZT$

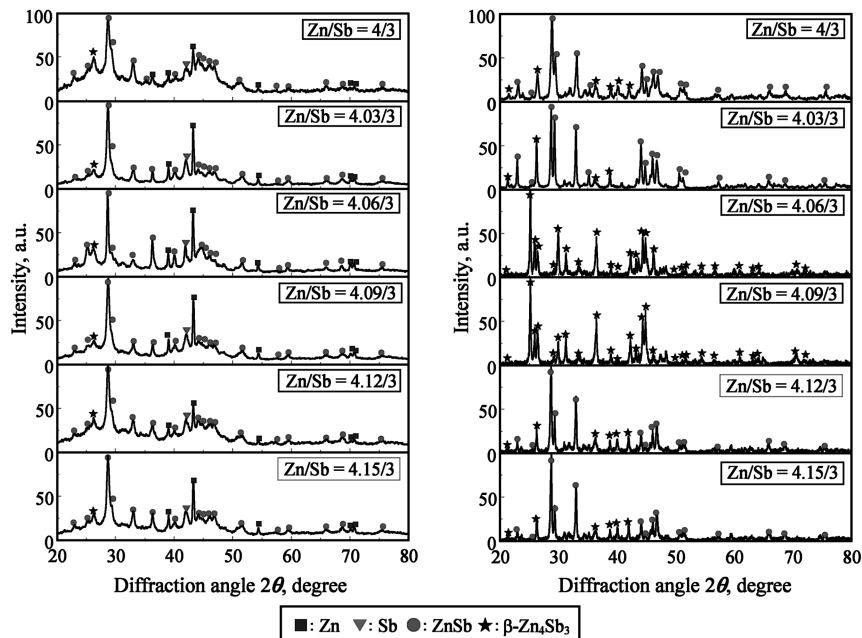


**Fig. 4** Influences of mole ratio Zn/Sb on x-ray diffraction patterns of MA powder and PDS-bulk material sintered at 723 K.

**Table 3 Principal phases synthesized under different conditions in mole ratio Zn/Sb**

Mole ratio Zn/Sb	4.03/3	4.06/3	4.09/3	4.12/3	4.15/3
MA powder	ZnSb + Zn	ZnSb + Zn	ZnSb + Zn	ZnSb + Zn	ZnSb + Zn
PDS-bulk material at 673 K	N.A.	N.A.	ZnSb + Zn	N.A.	N.A.
PDS-bulk material at 723 K	ZnSb	$\beta$ -Zn <sub>4</sub> Sb <sub>3</sub>	$\beta$ -Zn <sub>4</sub> Sb <sub>3</sub>	ZnSb	ZnSb

defined with Eq. (1) is a useful index of thermoelectric performance. Figure 11 shows the temperature dependencies of the thermoelectric figure of merit for the samples sintered at the different temperatures. The sample sintered at 723 K has the maximum  $ZT$  of 1.17 at the measurement temperature of 673 K. This leads to high thermoelectric performance.

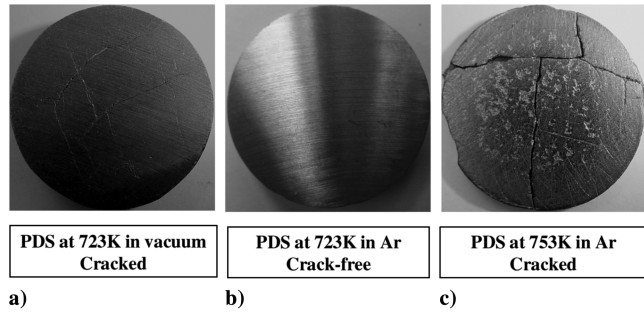


**Fig. 5 Outward appearance pictures of samples sintered under different conditions.**

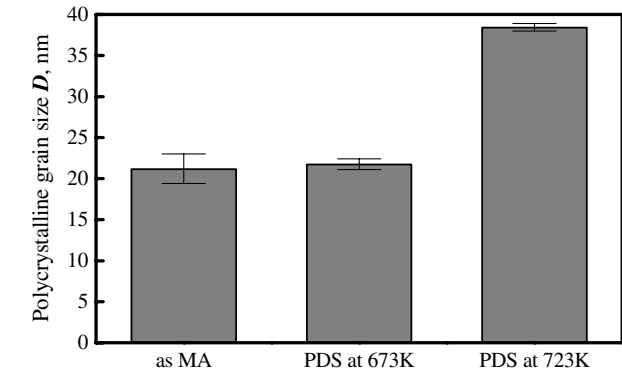


**Fig. 6 Change in polycrystalline grain size at different sintering temperatures.**

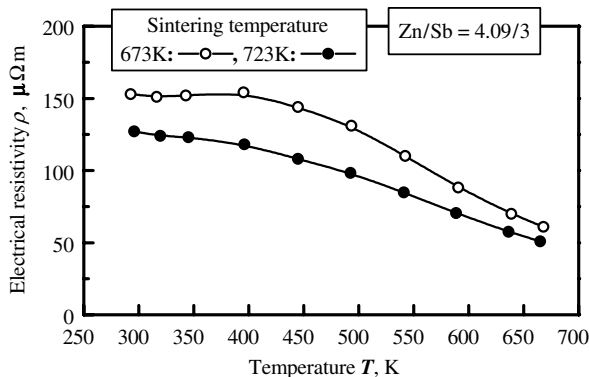


**Fig. 7 Comparison between electrical resistivities of two samples sintered at different temperatures.**

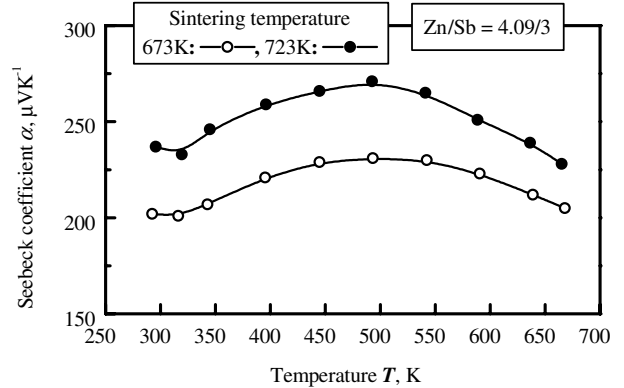


**Fig. 8 Comparison between Seebeck coefficients of two samples sintered at different temperatures.**

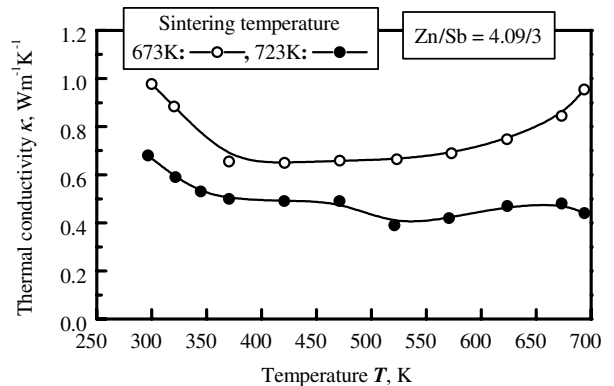


**Fig. 9 Comparison between thermal conductivities of two samples sintered at different temperatures.**

**IV. Conclusions**

The synthesis of  $\beta$ -Zn<sub>4</sub>Sb<sub>3</sub> compound was attempted by using the MA-PDS method. The results obtained in this study are summarized as follows.

1) In the samples mixed with mole ratio Zn/Sb of 4/3 and milled for 50 to 300 h, the ZnSb compound is easily synthesized by PDS at 723 K.

2) The polycrystalline grain size of the sample powder with mole ratio Zn/Sb = 4/3 decreases with the milling time up to 75 h and it becomes about 15 nm in the milling time longer than 75 h. The minimum polycrystalline grain size after PDS is obtained in the milling time of around 100 h.

3) For making a sound sintered body, the compacted powder should be sintered at 673 or 723 K in argon atmosphere.

4) The  $\beta$ -Zn<sub>4</sub>Sb<sub>3</sub> compound can be synthesized from the powder mixed with the mole ratio Zn/Sb of 4.06/3 or 4.09/3 and milled for 100 h by sintering at 723 K.

5) The  $\beta$ -Zn<sub>4</sub>Sb<sub>3</sub> compound exceeds the mixture of ZnSb and Zn in all the thermoelectric properties (namely, the electrical resistivity, the Seebeck coefficient, and the thermal conductivity) and leads to the good thermoelectric performance.

6) The high-performance thermoelectric compact  $ZT > 1$  can be produced under the conditions of the optimum mole ratio of mixed powder and high sintering temperature (723 K).

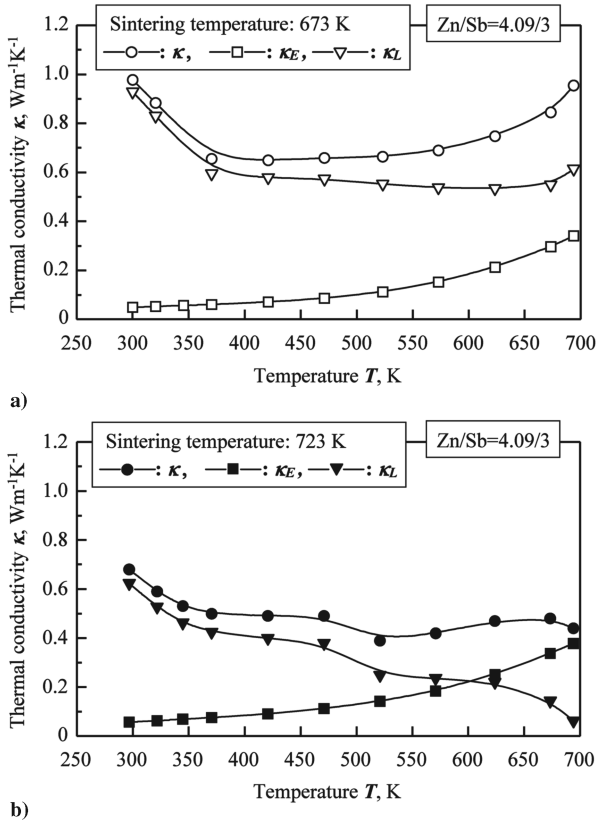


Fig. 10 Three types of thermal conductivities of two samples sintered at different temperatures.

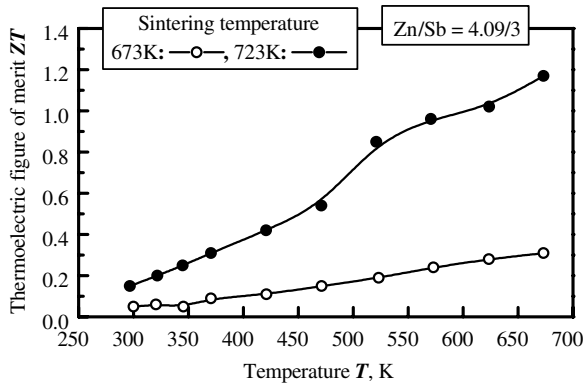


Fig. 11 Comparison between thermoelectric figures of merits of two samples sintered at different temperatures.

## Acknowledgment

This work was supported by a Grant-in-Aid for Scientific Researches from the Ministry of Education, Culture, Sports, Science and Technology, Japan (no. 16656298).

## References

- [1] Soma, T., Nakamoto, T., and Kuru, M., "Thermoelectric Properties in Low Temperature of  $Zn_4Sb_3$  Compounds," *Proceedings of TEC2001*, The Thermoelectric Society of Japan, Tokyo, 2001, pp. 52–53.
- [2] Caillat, T., Fleurial, J.-P., and Borschhevsky, A., "Preparation and Thermoelectric Properties of Semiconducting  $Zn_4Sb_3$ ," *The Journal of Physics and Chemistry of Solids*, Vol. 58, No. 7, 1997, pp. 1119–1125. doi:10.1016/S0022-3697(96)00228-4
- [3] Yamamoto, J., Fukagawa, K., Iwaisako, K., Lee, T., Takazawa, H., Ohta, T., Ueno, K., Sugaya, Y., and Aizawa, T., "Thermoelectric Properties of  $\beta$ - $Zn_4Sb_3$  Made by Bulk Mechanical Alloying," *Proceedings of TEC2000*, The Thermoelectric Society of Japan, Tokyo, 2000, pp. 40–41.
- [4] Ohzora, Y., Nagai, J., Hayashi, H., and Fujii, K., "Production of  $\beta$ - $Zn_4Sb_3$  Having High Thermoelectric Properties and High Mechanical Properties," *Proceedings of TEC2002*, The Thermoelectric Society of Japan, Tokyo, 2002, pp. 24–25.
- [5] Zhang, L. T., Tsutsui, M., Ito, K., and Yamaguchi, M., "Effects of ZnSb and Zn Inclusions on the Thermoelectric Properties of  $\beta$ - $Zn_4Sb_3$ ," *Journal of Alloys and Compounds*, Vol. 358, Nos. 1–2, 2003, pp. 252–256. doi:10.1016/S0925-8388(03)00074-4

A. Gupta  
Associate Editor